Biochemical Engineering Journal 141 (2019) 80–88

Contents lists available at ScienceDirect

Biochemical Engineering Journal

journal homepage: www.elsevier.com/locate/bej

Regular article

BSA/ASN/Pol$_{407}$ nanoparticles for acute lymphoblastic leukemia treatment

Ana Tinoco[a], Marisa P. Sárria[b], Ana Loureiro[a], Pier Parpot[c], Begoña Espiña[b], Andreia C. Gomes[d], Artur Cavaco-Paulo[a], Artur Ribeiro[a,*]

[a] CEB-Centre of Biological Engineering, University of Minho, Campus de Gualtar, 4710-057, Braga, Portugal
[b] INL - International Iberian Nanotechnology Laboratory, Braga, Portugal
[c] Centre of Chemistry, Department of Chemistry, University of Minho, CBMA, 4710-057, Braga, Portugal
[d] Centre of Molecular and Environmental Biology (CBMA), Department of Biology, University of Minho, 4710-057, Braga, Portugal

HIGHLIGHTS

- BSA/ASN/Pol$_{407}$ nanoparticles production by high pressure homogenization.
- Stable nanoparticles with suitable properties for intravenous applications.
- BSA/ASN/Pol$_{407}$ nanoparticles hydrolyze asparagine retaining the ammonia produced.
- Immobilization decreases the negative effect of free asparaginase on zebrafish.
- The ZET assay supports the safety of the BSA/ASN/Pol$_{407}$ formulations.

ARTICLE INFO

Keywords:
Asparaginase
Nanoparticle
Acute lymphoblastic leukemia
Hyperammonemia
Ammonia retention
ZET assay

ABSTRACT

During the treatment of acute lymphoblastic leukemia (ALL) with asparaginase (ASN) there is an accumulation of ammonia in the body as result of asparagine hydrolysis. This accumulation known as hyperammonemia is one of the main side-effects of this therapy. To avoid hyperammonemia is urgent to develop new strategies for ammonia retention. Herein is presented the immobilization of ASN into bovine serum albumin/poloxamer 407 (BSA/Pol$_{407}$) nanoparticles. The ability of the developed nanoparticles to hydrolyze asparagine while retaining the forming ammonia is also explored. Different percentages of ASN were entrapped into BSA nanoparticles coated with Poloxamer 407 and were prepared by high-pressure homogenization. The nanoparticles were characterized regarding their physico-chemical properties, stability, capacity to retain ammonia and safety using zebrafish embryos as an *in vivo* model of toxicity. The BSA/ASN$_{25\%}$/Pol$_{407}$ nanoparticles were selected as the best formulation to hydrolyze asparagine using the lowest nanoparticle concentration. These nanoparticles presented physical characteristics suitable for an intravenous application and were capable to retain the forming ammonia decreasing the negative effect of free ASN on zebrafish survival. These nanoparticles could potentially be used to prevent hyperammonemia during ALL treatment with ASN.

1. Introduction

Acute lymphoblastic leukemia (ALL) is a malignant cancer of the blood and bone marrow, affecting the white blood cells responsible to fight infections. This disease is characterized by an uncontrolled increase and excessive multiplications of malignant and immature lymphoblast in bone marrow. It alters the normal blood cells function and, in many instances, can lead to death [1,2]. Among the antitumor drugs used for the ALL treatment, there is one chemotherapeutic agent in pediatric oncotherapy specific for ALL that is the bacterial enzyme asparaginase. This enzyme has been employed as the most effective chemotherapeutic agent in pediatric ALL and improved the survival rate of pediatric ALL to approximately 90% in recent trials [3].

Asparaginase (ASN) belongs to an amidase group responsible for the hydrolysis of the amide bond in asparagine, forming aspartic acid and ammonia. This catalysis reaction is responsible for ASN's antileukemic activity because normal cells are able to synthesize asparagine while leukemic lymphoblasts are sensitive to the depletion of this extracellular amino acid [4,5]. Malignant cells either express low levels of asparagine synthetase or lack the capacity to upregulate the expression of this enzyme in the absence of serum asparagine. Therefore, administration of ASN leads to asparagine depletion, inhibiting protein and

* Corresponding author.
E-mail addresses: arturibeiro@ceb.uminho.pt, artur@bio.uminho.pt (A. Ribeiro).

https://doi.org/10.1016/j.bej.2018.10.006
Received 20 April 2018; Received in revised form 25 September 2018; Accepted 8 October 2018
Available online 09 October 2018
1369-703X/

RNA synthesis, which results in starvation and cancer cell death [6,7]. However, there are several side effects associated with this therapy like hyperammonemia, defined by serum ammonia levels above 50 μmol/L in the absence of liver disease [8–10]. Currently, hyperammonemia is treated by reducing blood nitrogen levels by lower exogenous nitrogen intake through protein restriction, by hemodialysis or ammonia-trapping therapy with sodium benzoate and sodium phenylacetate [9]. In this way, it is important to develop new strategies to avoid this side-effect, like asparaginase entrapment into protein nanoparticles.

Previously, we reported the ability of albumin/asparaginase capsules prepared by ultrasound to retain ammonia [11]. Despite the positive results, the nanoparticles physical properties were not suitable for an intravenous administration and thus an improvement was essential regarding the intended application. In this work we present different BSA/ASN/Pol_{407} formulations, prepared by high-pressure homogenization (HPH), which were optimized for asparaginase entrapment. Using HPH we aimed to obtain monodisperse particles with sizes close to 100 nm, ideal for an intravenous application. The nanoparticles were optimized relatively to enzyme concentration, asparaginase addition during nanoparticles preparation and toxicity using an *in vivo* model.

BSA is a protein extensively used in drug delivery systems due to several characteristics that include nontoxicity, nonimmunogenicity, biodegradability and low cost. For this system, BSA show ideal features since albumin nanoparticles allow electrostatic adsorption of charged molecules due to the charged amino acids at the nanoparticles surface. Also, this nanoparticles can be chemically functionalized due to the reactive groups located at the nanoparticles surface [12,13]. The incorporation of Pol 407 in the formulations allows the production of PEGylated nanoparticles without additional chemical surface modification. It is described that PEGylated nanoparticles exhibit reduced adsorption of blood opsonins and consequently resist to the ingestion by phagocytic scavenger cells, promoting their long blood circulation time and biodistribution [14].

HPH is frequently used to obtain particles with small size and high stability [15]. During the HPH process, the liquid is forced to pass through a thin gap under high pressure. Thus, it leads to fast acceleration and, as the fluid exits the homogenization valve, the pressure suffers an extreme pressure drop. The effects caused by the HPH cannot be produced by one single physic phenomenon. At high pressure, it involves a combination of high hydrostatic pressure, shear stress, cavitation collapse, strong impacts, high-speed friction and heating that are responsible for emulsion formation [16]. The mechanical force involved in the HPH process can cause structural changes and denaturation of proteins while is able to disrupt the oil droplets into uniform dispersion, adsorbing the denatured proteins into the oil droplets surface. The high shear forces are able to modify protein conformation by affecting intramolecular hydrogen, hydrophobic and electrostatic interactions and it alters the tertiary and/or quaternary structure of most globular proteins with relatively low influence on their secondary structure. This method is able to disrupt the disulfide bonds in protein molecules and the new disulfide bonds are formed by cysteine of intra- and inter- albumin molecules. These formulations are electrostatically stabilized due to the repulsion forces between the nanoparticles since all nanoparticles are negatively charged in the dispersing media [14]. The BSA/ASN/Pol_{407} nanoparticles produced by HPH were characterized with respect to their stability, physical properties, *in vivo* toxicity and capacity to retain ammonia. The new BSA/ASN/Pol_{407} nanoparticles will potentially have the capacity to simultaneously increase enzyme stability over time in order to decrease the number of intravenous administrations, while retaining the free ammonia resulting from asparaginase activity (Scheme 1). The ammonia retention on the nanoparticles interface could result from the electrostatic interaction between the positively charged ammonia and the superficial negatively charged groups of the nanoparticles; and from the entrapment of ammonia in the surface of the nanoparticles.

The BSA/ASN/Pol_{407} nanoparticles along with the adsorbed ammonia are expected to be cleared from the body by the mononuclear phagocyte system [17]. It was already demonstrated by some authors the capacity of albumin particles to be phagocytosed by cells of the mononuclear phagocyte system and completely degraded within 7 days [18].

2. Materials and methods

2.1. Chemicals and reagents

ASN was obtained from Changzhou Qianhong BioPharma Co., Ltd. (Jiangsu, China). Asparagine, aspartic acid, and Pol 407 were obtained from Sigma (USA). BSA and Nessler reagent were obtained from Sigma-Aldrich (USA). All other chemicals including eluents for high performance liquid chromatography-mass spectrometry (HPLC-MS) and salts were of analytical reagent grade.

2.2. BSA-based nanoparticles prepared by high pressure homogenization

The preparation of BSA/ASN/Pol_{407} nanoparticles was achieved by emulsification using high-pressure homogenization [15]. All the components were dissolved in phosphate buffered saline (PBS) 1x, pH 7.4, with a final protein concentration (BSA plus ASN) of 10 mg/mL and emulsified with 0.5% (v/v) vegetable oil by subjecting the mixture to 26 cycles of high pressure homogenization (240 and 580 bar). The PEGylated nanoparticles were composed by Pol_{407} on a concentration of 5 mg/mL and a percentage of enzyme varying from 5 to 25% (w/w) relatively to the BSA concentration. The enzyme was added to the formulation after 5 homogenization cycles. The nanoparticles were collected by centrifugation using Vivaspin® 6 (Sartorius, Germany) provided of a membrane with a molecular weight cut-off of 300.000 Da.

To characterize the immobilization process for the different formulations, two parameters were evaluated: nanoparticles formation efficiency and nanoparticles encapsulation efficiency [11]. For both parameters, only the protein in the aqueous phase, obtained after nanoparticles centrifugation, was used for quantification. For nanoparticles formation efficiency, the proteins in the aqueous phase was quantified by Lowry method using the formula:

$$Formation\ effieciency\ (\%) = \frac{[Protein]_{total} - [Protein]_{free}}{[Protein]_{total}} \times 100$$

where $[Protein]_{total}$ and $[Protein]_{free}$ is the total concentration of protein added in formulation and the free concentration of protein in the aqueous phase solution after centrifugation, respectively.

For the encapsulation efficiency, the aqueous phase was analyzed by SDS-PAGE, using a 12.5% acrylamide/bis-acrylamide gel, and the bands of free asparaginase identified. The gel was then examined with the image process software ImageJ 1.50i. Comparing the intensities of the molecular marker bands and the bands of asparaginase monomer, it was possible to determine the relative intensity per μg of protein and calculate the encapsulation efficiency [19].

2.3. Nanoparticle characterization

The nanoparticles were dispersed in PBS 1×, pH 7, and analyzed at 25 °C for their size distribution and polydispersity index (PdI). For the Z-potential analysis, the same conditions were used with the nanoparticles dispersed in ultra-pure water. The parameters were determined by photon correlation spectroscopy, using dynamic light scattering (DLS) (Malvern Instruments, Nano-ZS) [11]. The values for viscosity and refractive index were 0.8872 cP and 1.330, respectively. Each sample was measured in triplicate and the results are presented as mean value ± standard deviation (SD).

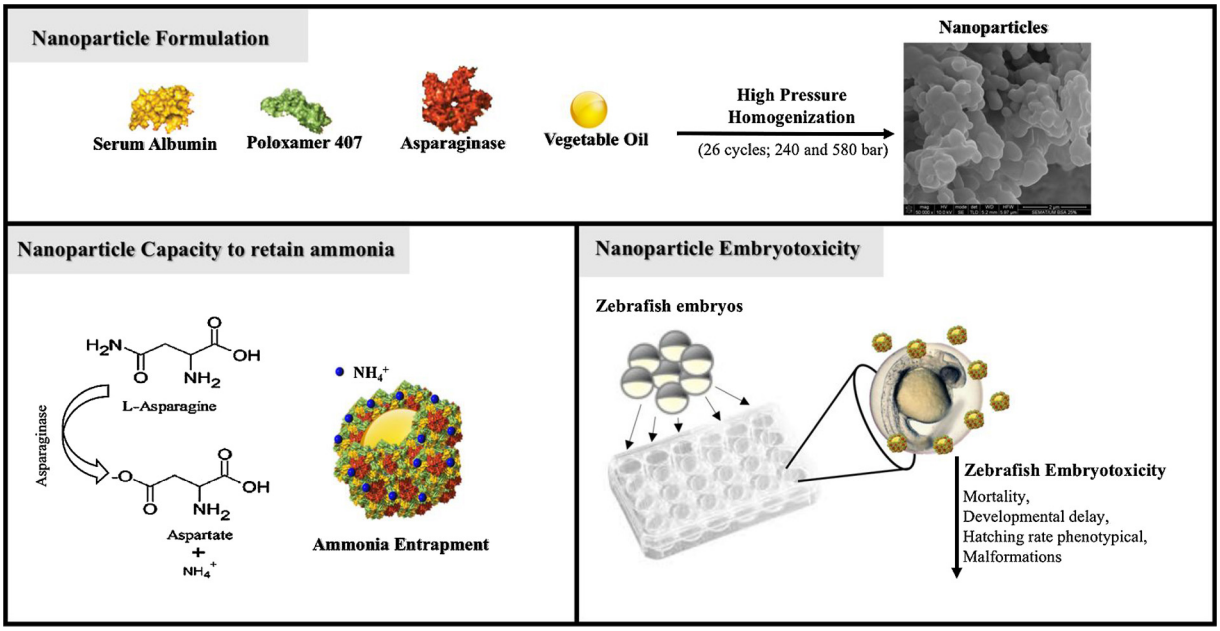

Scheme 1. BSA based nanoparticles for hyperammonemia prevention during acute lymphoblastic leukemia treatment with asparaginase.

2.4. Nanoparticles morphological characterization

The morphology of BSA/ASN/Pol_{407} nanoemulsions was evaluated by SEM and STEM analysis. For SEM the particles were coated with 80% Au and 20% Pd before observation at 5.0 kV. For STEM the diluted nanoemulsions suspension were dropped on copper grids with a 400 mesh carbon film, 3 mm in diameter. The shape and morphology of the microspheres were observed using a NOVA Nano SEM 200 FEI instrument.

2.5. Determination of ASN enzymatic activity

The hydrolysis reaction of asparagine was performed with 0.001 g/L of ASN or the corresponding concentration of immobilized enzyme and 100 mM of asparagine, at 37 °C, in 50 mM Tris − HCl, pH 8.0, or ultra-pure water, for 240 min. When the reaction was performed in ultra-pure water, the enzyme was inactivated on ice and removed from the medium by ultra-centrifugation (10,000 RCF, 30 min) in microtubes with a membrane cut-off of 5000 Da. After ultra-centrifugation, the membrane was washed with ultra-pure water to prevent amino acid retention in the membrane, and quantification of ammonia and aspartic acid was performed [11]. Ammonia quantification was determined by a stopped assay using Nessler's reagent. The ammonia produced in 10 µL of the reaction mixture was determined by adding 990 µL Nessler's reagent. The optical density of the solution was read at 436 nm (BioTek®, Synergi MX), and the ammonia concentration was determined on the basis of a standard curve previously obtained with ammonium sulfate as a standard [20,21].

2.6. Aspartic acid quantification by HPLC-MS without derivatization

2.6.1. Mass spectrometer method

Mass spectrometer analysis was performed on Finnigan LXQ mass spectrometer in a positive ionization mode. The aspartic acid solution was prepared in ultra-pure water with 20% of acetonitrile and then filtered with 0.2 µm filters. High flow source conditions were optimized for aspartic acid with a flow rate of 5 µL/min. Source voltage was 4.95 kV, and source current was 0.60 µA. Sheath gas, aux gas and sweep gas were 40, 20 and 19.98 arb, respectively. Capillary voltage was 17.77 V, capillary temperature was 274.88 °C and the tube lens voltage was 25.01 V [11].

2.6.2. HPLC-MS method

A reverse-phase HPLC-MS system with the column Synergi Hydro-RP, 80 Å, 4 µm and 150 × 4.60 mm (Phenomenex®) was used to isolate aspartic acid. As eluent, the selected solvent was ammonium bicarbonate 0.01 M with the pH adjusted to 6.0, with formic acid (A) and acetonitrile (B). A sample volume of 25 µL was injected with a flow rate of 0.3 mL/min for 20 min. The gradient program started with 95% solvent A during the first 8 min, decreased linearly to 40% solvent A in the next 7 min, and returned to the initial 95% during the next 5 min. In consequence, the solvent B started with 5% during the first 8 min, increased linearly to 60% solvent A in the next 7 min, and returned to the initial 5% during the next 5 min. The peak identification was performed through the MS detector and compared to the elution times obtained when the amino acids were analyzed separately, in the same conditions. For a more correct calculation of the peak area, the 'Base Peak' control from Xcalibur program was used. With this control, it is possible to obtain the peak from each amino acid individualized by selecting their mass weight [11].

2.7. ZET protocol and collected data

In vivo nanotoxicity and bioactivity of ASN enzyme, either free or immobilized in BSA/Pol_{407} nanoparticles, was assessed with the zebrafish embryo toxicity (ZET) assay, as described in Oliveira et al. 2016 [22]. All experiments were conducted in agreement with the applicable European legislation on animal welfare, *i.e.* Directive 86/609/EEC, which allows zebrafish embryos to be used up to 120 h post-fertilization (hpf). As the ZET experiments were carried out up to 56 hpf, no license was required.

Zebrafish zygotes within 2 hpf were randomly allocated into 24-well microplates (5 eggs per mL), with continuous waterborne exposure of free and immobilized ASN at different concentrations (7 and 70 µg/mL), for 56 hpf. All the ASN solutions were prepared in autoclaved PBS 1x, pH 7.4, filtered with 0.22 µm polystyrene membrane and pre-warmed before application. Stock solutions were kept overnight at 4 °C and re-warmed for solution renewal prior use at 24 and 48 h of incubation. All zebrafish embryos were derived from the same eggs spawn. Autoclaved and filtered (*via* 0.22 µm polystyrene membrane)

freshwater was used in all treatments, obtaining a zebrafish embryonic maximum mortality of 25% in the control group. To ensure optimal incubation temperature of the zebrafish embryos, all the test solutions and suspensions were pre-heated to 28 ± 1 °C. To investigate the effect of ASN exposure on zebrafish embryos, survival rates were investigated and multiple sub-lethal parameters were collected. Morphometrically, the chorion and yolk volumes were measured at 8 and 32 hpf. In addition, the head-trunk angle (HTA) of 32 hpf zebrafish embryos was measured in order to detect atypical straightening [23]. 20 embryos from each test condition (10 per quadruplicates) were randomly selected and the number of heart beats were counted during 10 s at 32 and 56 hpf. In order to avoid bias, "blind" observations were performed by a single person. At 8, 32 and 56 hpf, 20 zebrafish embryos from each condition were photographed using a Nikon Eclipse TS 100 inverted microscope with Nikon digital sight camera DS-Fi1. All morphometric analysis was performed using the image processing program ImageJ 1.46 r. The following developmental endpoints were further assessed: developmental delay, phenotypical malformations and hatching rate. In all ZET experiments, dead embryos were removed to avoid cross-contamination, a process repeated three times every 24 h [24].

2.7.1. Zebrafish embryogenesis statistical analysis

All assumptions were met prior to data analysis. Shapiro-Wilk test was used for normality evaluation and Levene's test was applied for homogeneity of variances certification. To investigate differences among ASN concentrations in the overall survival of zebrafish embryos, a chi-square test was performed with the observed values for each test condition. The null hypothesis of "no differences among ASN concentrations" was assumed for the consideration of the expected values (average survival of all treatments, for a given hpf). The effect of ASN exposure on egg volume (8 hpf), head-trunk angle (32 hpf) and heart rate (32 hpf and 56 hpf) of zebrafish embryos, was evaluated through a six-level one-way ANOVA analysis. In order to test for differences among ASN concentrations on zebrafish embryos hatching rate (56 hpf), a chi-square analysis was conducted. The null hypothesis of "no differences among ASN concentrations" was considered for the establishment of the expected values (average hatching rate of all treatments). To avoid biases associated with covariates, ANCOVA model was applied to determine the influence of ASN on zebrafish embryos yolk volume (8 hpf and 32 hpf; egg volume was used as co-variable) and yolk extension (56 hpf; body length was used as co-variable). Post hoc comparisons were conducted using Student-Newman-Keuls. A P value of 0.05 was used for significance testing. Analyses were performed in STATISTICA (StatSoft v.7, US) [22].

3. Results

3.1. Effect of enzyme concentration on nanoparticles physical properties

To study the effect of enzyme concentration on nanoparticles physical properties (mean size, surface charge and size distribution), five different BSA/ASN/Pol_{407} nanoparticles were obtained varying ASN concentration in the nanoparticles formulation. Generally, a size below 75 nm was observed for all the formulations 1 day after synthesis (Table 1). The nanoparticles with smaller size (62.8 ± 1.41 nm) were obtained for the formulation containing 25% ASN, and the formulations with 15 and 25% of enzyme presented a more homogeneous population (PdI < 0.13). Relatively to the Z-potential, all formulations presented a surface charge close to neutrality. All formulations were characterized regarding their stability along time of storage and in Fig. 1 is represented the data regarding the most stable formulation – BSA/$ASN_{25\%}$/Pol_{407} – which was selected for further assays. This formulation was stable over time in terms of size and the measured PdI was always lower than 0.2, demonstrating the homogeneity of the formulation (Fig. 1-B). Regarding the Z-potential (Fig. 1-A), it was verified that the nanoparticles become more negative over time. For this formulation, the nanoparticle formation efficiency was 91.11 ± 1.6% and the encapsulation efficiency was 85.38 ± 1.5%. Encapsulation efficiency for the other BSA/ASN/Pol_{407} formulations ranged between 70 and 80% (Table 2). The small size of the BSA/$ASN_{25\%}$/Pol_{407} nanoparticles was confirmed by STEM analysis, which recorded a population diameter ranging between 87.5 and 134.1 nm (Fig. 2-A). These values are slightly higher than those measured with DLS (Table 1) which may result from differences between techniques. Also, using SEM technology (Fig. 2-B), it was also demonstrated the nanoparticles spherical shape.

Table 1
Physical properties of BSA/ASN/Pol_{407} nanoparticles one day after synthesis and 4 °C storage. The values were calculated and expressed as mean ± SD (n = 3).

Formulation	Size (nm)	PdI	Z-potential (mV)
BSA/$ASN_{5\%}$/Pol_{407}	71.11 ± 0.88	0.20 ± 0.00070	−2.13 ± 0.099
BSA/$ASN_{10\%}$/Pol_{407}	69.09 ± 0.67	0.19 ± 0.027	−1.28 ± 0.034
BSA/$ASN_{15\%}$/Pol_{407}	72.53 ± 1.15	0.11 ± 0.021	−0.33 ± 0.014
BSA/$ASN_{20\%}$/Pol_{407}	73.99 ± 3.74	0.23 ± 0.0028	−1.96 ± 0.078
BSA/$ASN_{25\%}$/Pol_{407}	62.80 ± 1.41	0.13 ± 0.010	−3.79 ± 0.20

3.2. Effect of enzyme concentration on BSA/ASN/Pol_{407} nanoparticles activity over time

ASN activity of all formulations was evaluated over the 4 months of storage at 4 °C, using the Nessler method that quantifies the produced ammonia in solution resulting from asparagine hydrolysis (Fig. 3). The starting values (*i.e.* 0 months) correspond to the activity determined one day after synthesis. As it is possible to observe in Fig. 3, ASN activity of immobilized enzyme was lower when compared to the free enzyme in PBS. After 1 month of storage, a 70% decrease in the activity of the free enzyme in PBS was verified. The formulation BSA/$ASN_{5\%}$/Pol_{407} showed 30% less hydrolytic activity, which is significant but less drastic when compared to the free enzyme. The remaining formulations either maintained or displayed increased enzyme activity over this period.

After 4 months of storage, the formulations with higher enzyme stabilization evaluated in terms of enzyme activity were those with higher ASN concentration, namely the formulations with 15, 20 and 25% of enzyme. These formulations can be stored up to 4 months at 4 °C while maintaining a high asparaginase activity. Considering the ASN activity over time and the nanoparticles physical properties, the BSA/$ASN_{25\%}$/Pol_{407} formulation was selected to study ammonia retention and *in vivo* toxicity. Also, with this formulation it will be possible to use lower nanoparticles concentration in order to achieve higher rates of asparagine hydrolysis.

3.3. Nanoparticles capacity to retain ammonia

The main objective of this work was the development of a new system capable to simultaneously hydrolyze the free asparagine from serum but also retain the ammonia formed during the hydrolysis reaction. In this way, two different concentrations of ASN, free or immobilized into BSA/$ASN_{25\%}$/Pol_{407} nanoparticles, were incubated with 100 mM asparagine in ultra-pure water at 37 °C, for 4 h. Then, the nanoparticles were removed from the reaction medium. The free ammonia was quantified using the Nessler reagent and the aspartic acid quantified by an HPLC-MS method developed previously by our group [11] - Table 3.

For this assay, two different concentrations of ASN (7 and 70 μg/mL) were tested. 70 μg/mL of ASN was chosen according to the highest BSA concentration (300 μg/mL) tested *in vivo via* a ZET assay (data not shown).

Analyzing Table 3, it is possible to note that almost all the asparagine in the medium was hydrolyzed when incubated with the

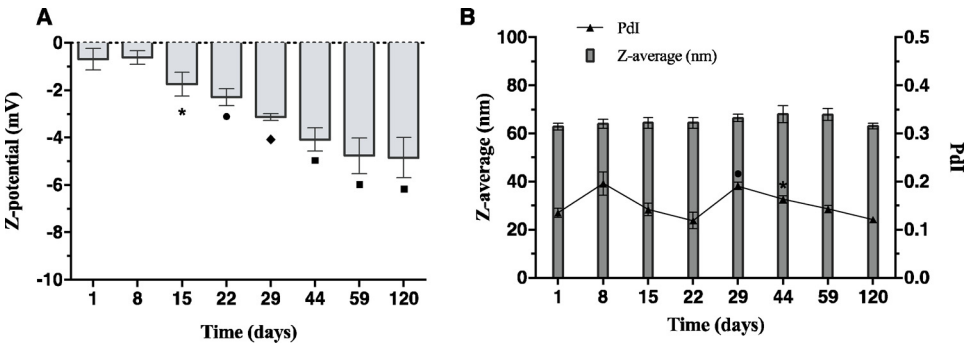

Fig. 1. Characterization of BSA/$ASN_{25\%}$/Pol_{407} nanoparticles during storage at 4 °C. a) Z-potential, b) Z-average and PdI. The data represents the mean ± SD from three independent experiments. Data were analyzed by one way-ANOVA: P-value ≤0.05 (asterisk), P-value ≤0.01 (circle), P-value ≤0.001 (diamond), P-value ≤0.0001 (square), compared to the results obtained at day 1.

Table 2
Nanoparticles formation efficiency and nanoparticles encapsulation efficiency. The values were calculated and expressed as mean ± SD (n = 3).

Formulation	Formation efficiency (%)	Encapsulation efficiency (%)
BSA/$ASN_{5\%}$/Pol_{407}	93.10 ± 0.58	70.33 ± 1.91
BSA/$ASN_{10\%}$/Pol_{407}	90.89 ± 0.98	82.48 ± 4.96
BSA/$ASN_{15\%}$/Pol_{407}	90.42 ± 1.35	81.85 ± 3.60
BSA/$ASN_{20\%}$/Pol_{407}	90.67 ± 1.97	72.77 ± 4.17
BSA/$ASN_{25\%}$/Pol_{407}	91.11 ± 1.60	85.38 ± 1.50

nanoparticles, which was not observed when testing free enzyme. It is thus possible to conclude that enzyme entrapment leads to a higher activity when compared to the free enzyme due to its stabilization by the system. Relatively to the ratio aspartic acid/ammonia, this ratio was above 1 only with nanoparticles, which indicates that the ammonia is retained in the nanoparticles.

3.4. *In vivo toxicity evaluation of ASN nanoparticles using the ZET protocol*

Zebrafish embryos represent an attractive model for preclinical drug discovery applications since they offer the possibility to perform small-scale high-throughput analyses [25]. The main advantages of using zebrafish embryos for compound screening are their rapid development, small size, easy maintenance, transparency and capacity to absorb compounds dissolved in the water [26]. Zebrafish embryos are thus used as a powerful, alternative model for toxicity testing to provide an *in vivo* assessment of new compounds and nanoparticles at an early stage in drug discovery [27,28]. Taking in account all these characteristics, zebrafish embryos were used as a model to test the BSA/ASN/Pol_{407} nanoparticles toxicity.

Controls for this experiment (effect of the free compounds that compose the nanoparticles) were included and no significant differences were observed relatively to the control of untreated zebrafish embryos (data not shown). For simplicity, in this section, the free enzyme will be represented by ASN and the BSA/$ASN_{25\%}$/Pol_{407} nanoparticles by Np.

When analyzing the effects of ASN, free or immobilized in Np, on zebrafish embryos survival (Fig. 4), a significant interaction was observed among different groups for a given hpf ($\chi 2 = 12.266$; $DF = 4$; $P < 0.05$). The significant difference for the Np 7μg/mL is due to an increase in the zebrafish embryos' survival rate, pointing that the ASN entrapment into BSA/ASN/Pol_{407} nanoparticles decreased the toxic effect observed for the free enzyme. The time-window from 8hpf to 32hpf showed an increased zebrafish embryotoxicity for all conditions tested, including control (see Fig. 4), with all the conditions with a survival rate higher than 55%. The overall survival of zebrafish eleutheroembryos (embryos post-hatch, but prior to external feeding *i.e.* at 56 hpf) did not vary significantly from the survival rate exhibited at developmental stages immediately prior to hatching (*i.e.* 32 hpf).

Taking only into account the egg volume (Fig. 5-C), a decrease was detected at 32 hpf for the ASN 70 μg/mL and Np 7 μg/mL, although not statistically relevant. In this way, none of the tested conditions showed significant differences on egg volume during embryonic development ($F(4131) = 1.1031$, $P = 0.35793$).

In addition, an acceleration of the zebrafish embryonic hatching rate was verified at 56hpf for all the tested conditions ($\chi 2 = 13.270$; $DF = 4$; $P < 0.05$) (Fig. 5-F). It is important to notice that the results for Np 7 μg/mL and Np 70 μg/mL are equal, so the graphic overlaps for these two conditions.

When considering the effects of free and immobilized ASN on zebrafish head-trunk angle, no significant interaction between the considered factors was observed ($F(4.33) = 0.689$, $P = 0.60450$). Although not significant, a slightly decrease was observed in the head-trunk angle when incubated with higher concentration of free ASN. This did not occur when the enzyme was immobilized into the nanoparticles, which lead to a profile similar to the control group (Fig. 5-D).

Yolk extension is a developmental module formed in the phylotypic period of zebrafish embryogenesis, overlapping trunk straightening at

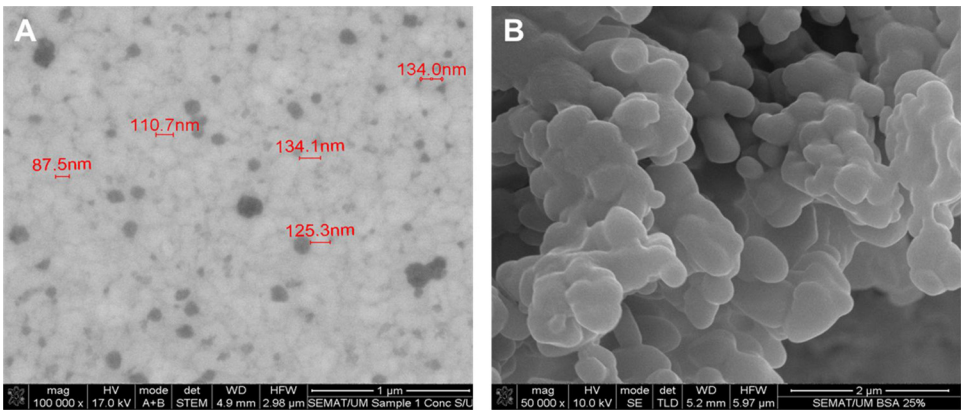

Fig. 2. STEM picture of BSA/$ASN_{25\%}$/Pol_{407} nanoparticles at 100000× (A); SEM picture of BSA/$ASN_{25\%}$/Pol_{407} nanoparticles at 50000× (B).

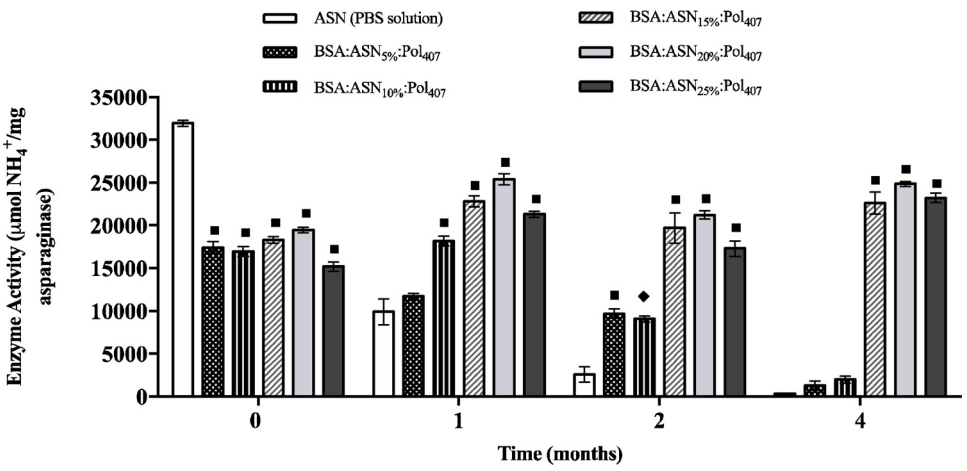

Fig. 3. Activity of free ASN in PBS and immobilized on BSA/ASN/Pol_{407} nanoparticles prepared by high pressure homogenization. Activity was determined for 4 months during storage at 4 °C. The reaction was performed with 0.001 g/L of ASN and 100 mM of asparagine for 240 min, at 37 °C, in 50 mM Tris-HCl, pH 8.6. Absorbance of the solutions after Nessler method was measured at 436 nm and compared with the absorbance of a calibration curve (Absorbance = 0.03598 [ammonia] mM). The data represents the mean ± SD from three independent experiments. Data were analyzed by one way-ANOVA: P-value ≤0.001 (diamond), P-value ≤0.0001 (square), compared to the results obtained for the free enzyme in PBS.

Table 3
Evaluation of ammonia retention by BSA/ASN25%/Pol407 nanoparticles. The values were calculated and expressed as mean ± SD (n = 3).

Samples	[Aspartic Acid][a] mM	[Ammonia][b] mM	Ratio [aspartic acid]/[ammonia]
BSA/$ASN_{25\%}$/Pol_{407} (ASN 7 µg/mL)	98.64 ± 2.30	97.31 ± 1.15	1.01
BSA/$ASN_{25\%}$/Pol_{407} (ASN 70 µg/mL)	99.78 ± 1.99	84.29 ± 2.99	1.19
ASN free (7 µg/mL)	89.47 ± 7.71	91.89 ± 1.91	0.97
ASN free (70 µg/mL)	93.91 ± 4.75	97.74 ± 0.12	0.96

[a] Aspartic acid quantified by HPLC-MS comparing the peak area with the calibration curve: Peak area = -2.26x10^5 ([aspartic acid] ^{2}mM) + 7.62x106 [aspartic acid] mM.
[b] Ammonia quantified by Nessler method considering the calibration curve: Absorbance = 0.0309 [ammonia] mM.

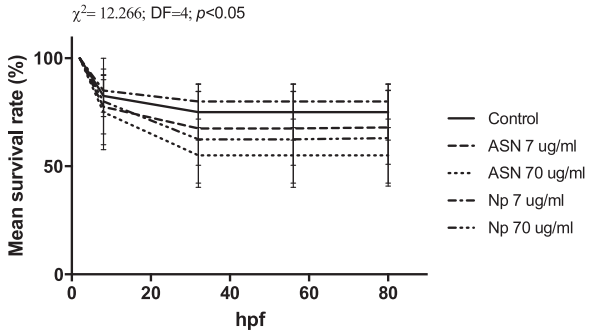

Fig. 4. The effects of ASN as free drug (ASN) and BSA/$ASN_{25\%}$/Pol_{407} nanoparticles (Np) exposure on *Danio rerio* embryos survival. Results shown are means of quadruplicate wells ± SD. Error bars represent the coefficient of variation for the findings.

the pharyngula stage [29]. When analyzing the effects of ASN in zebrafish embryos yolk extension (adjusted for total body length), it was verified that the presence of free or immobilized ASN tended for a relative increase of the yolk extension, with a significant increase for the ASN 70 µg/mL and Np 7 µg/mL ($F(4, 50) = 2.849$, $P < 0.05$) (Fig. 5-B).

ANCOVA results on effects of ASN free or immobilized in Np on zebrafish embryos yolk volume (adjusted for egg volume) showed no significant interaction among groups ($F(4130) = 1.0101$, $P = 0.40473$), independently of the hpf (Fig. 5-A).

Increased heart rate of zebrafish embryos (Fig. 5-E) was observed from 32 hpf to 56 hpf, which is expected during normal heart development [23]. Nested ANOVA results on effects of ASN (free and immobilized in Np) on zebrafish embryos heart rate showed no significant interactions for each tested time point in relation to the control group (32 hpf: one way ANOVA: $F(4, 44) = 0.72812$, $P = 0.57756$; 56 hpf: one way ANOVA: $F(4, 42) = 1.4972$, $P = 0.22033$). At 32 hpf, it was verified a slightly increase for the lowest concentration of immobilized ASN, although the differences are not statistically significant ($F(444) = 0.728$, $P = 0.57756$). For the 56 hpf, it was verified a small decrease on zebrafish embryonic heart rate for the highest concentration of free ASN, but the interaction was not significant ($F(442) = 1.497$, $P = 0.22033$).

4. Discussion

In order to develop a new strategy to retain the free ammonia forming during asparagine hydrolysis, different formulations with immobilized asparaginase were developed and characterized. All the formulations presented, at day 1, a small size (lower than 75 nm) which is an advantage for intravenous application [30] and an improvement when comparing with the BSA/$ASN_{2\%}$/Pol_{407} previously obtained by ultrasounds [11]. Relatively to the Z-potential, all the formulations demonstrated a superficial charge close to neutrality, what was expected due to the incorporation of Pol 407, a non-ionic surface active compound that exhibits a tendency to accumulate at the interface between the aqueous and organic phase, stabilizing the system [15]. This co-polymer is responsible for the nanoparticle's coating, which shields the surface charge [31].

The BSA/$ASN_{25\%}$/Pol_{407} formulation was selected for further assays because it permits to use a lower concentration of nanoparticles to attain a defined enzyme activity. This in turn reduces the risk of a potential toxic effect. Also, this formulation was stable in terms of size and PdI for more than 4 months when stored at 4 °C. When analyzed the Z-potential, it was verified that the nanoparticles become more negative over time, which could result from the desorption of some Pol 407 molecules from their surface [11]. Pol 407 is a non-anionic surfactant that forms a matrix with the BSA surrounding the oil phase. The removal of some molecules from the nanoparticle surface will shift the Z-potential to more negative values [15]. The formulation's ideal properties for intravenous application was corroborated by STEM and SEM analysis where it was confirmed the small size of BSA/$ASN_{25\%}$/Pol_{407} nanoparticles as well as its spherical shape, another positive feature for the intended application.

For the effect of enzyme concentration on BSA/ASN/Pol_{407} nanoparticles activity over time, it was verified that the activity of asparaginase immobilized into the nanoparticles was lower when compared to the free enzyme in PBS. This could be related to the harsh conditions

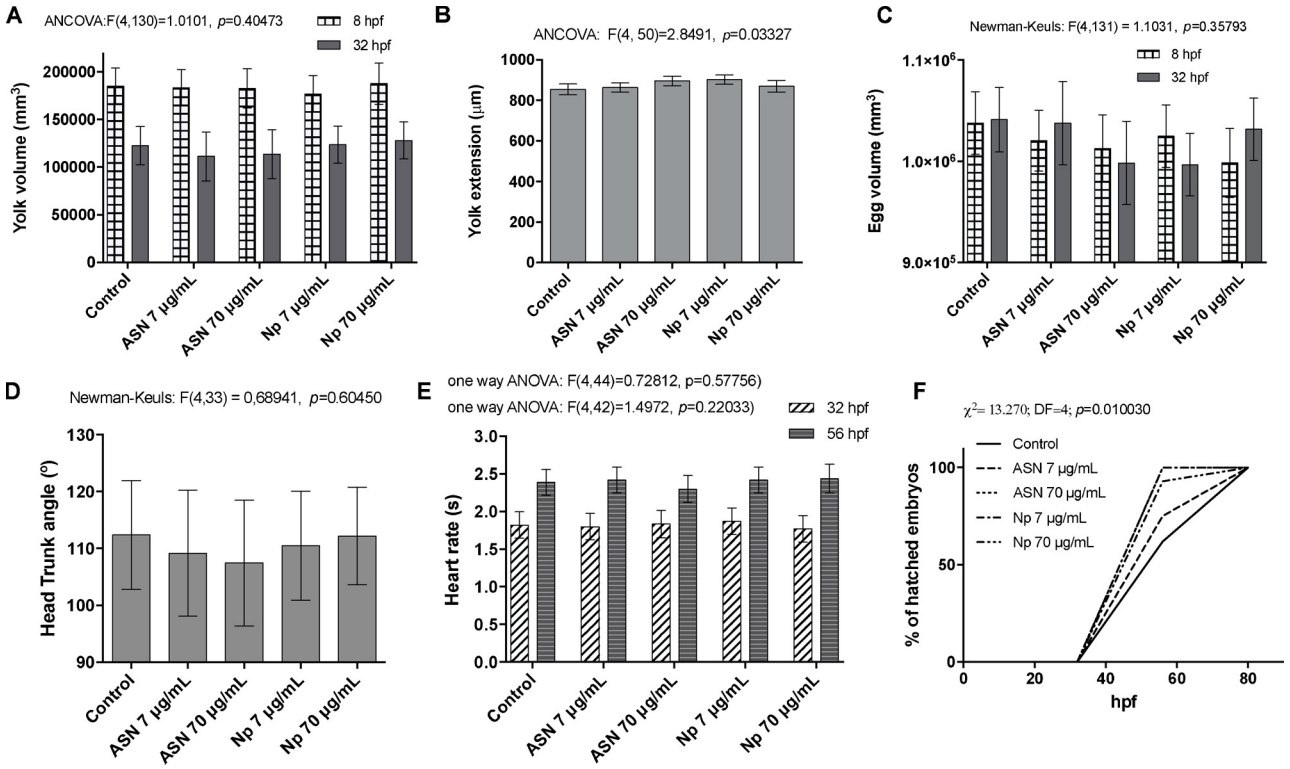

Fig. 5. The effects of ASN as free drug (ASN) and BSA/$ASN_{25\%}$/Pol_{407} nanoparticles (Np) exposure on *Danio rerio* embryos': A) yolk volume; B) yolk extension; C) egg volume; D) head trunk angle; E) heart rate and F) hatching rate. Results shown are means of quadruplicate wells ± SD. Error bars represent the coefficient of variation for the findings in the replicate wells.

employed during the homogenization process (high pressure and a temperature nearing 50 °C), with diffusional problems between the substrate and the enzyme, with steric hindrance blocking enzyme access to the substrate, with the loss of enzyme conformational freedom or due to the retention of ammonia on the particles surface [32,33]. After 1 month of storage, some formulations exhibited an increase on asparaginase activity associated with the stabilization of the nanoparticles or the loss of some Pol_{407} molecules from the nanoparticles surface, corroborated by the more negative values of the nanoparticles Z-potential. The loss of the Pol_{407} molecules could facilitate access to the substrate which would result in increased enzyme activity.

The BSA/$ASN_{25\%}$/Pol_{407} nanoparticles were studied regarding their capacity to retain ammonia and a ratio of aspartic acid/ammonia higher than 1 was verified which supports their capacity to retain ammonia. The capacity to retain the forming ammonia could be due to a conjugation of several phenomena: electrostatic interactions between the positive charge of ammonia and the negative charge on nanoparticles interface and the retention of ammonia on nanoparticles surface. In this way, the ammonia will be preferentially entrapped into the nanoparticles, rather than free in the serum. It is important to refer that, for this assay, were used enzyme concentrations much higher than the ones used in the determination of enzyme activity' for free or immobilized asparaginase – Fig. 3. Generally, all the substrate was hydrolysed within the 4 h of incubation and the differences between the free and immobilized asparaginase at month 0 were not verified.

To evaluate the BSA/$ASN_{25\%}$/Pol_{407} nanoparticles *in vivo* toxicity, zebrafish embryos were selected as a model. Taking in account all the advantages of this model [34], zebrafish can also be used as a model to study hyperamonemmia since its pathophysiology appears to be similar to that in mammals. Moreover, zebrafish brains cells appear to be as sensitive to ammonia as the human brain, so they are suitable to study drugs that can act as a neuro-protector against ammonia [35]. During embryonic stages, urea production has an important role in protecting the embryo from toxic effects of ammonia produced from a highly nitrogenous yolk. Also, in embryos, ammonia excretion is limited by the chorion so fish must detoxify ammonia by synthesizing urea [36,37]. All this similarities with mammals could be an indication of how zebrafish embryos could be used as a model to study the nanoparticles capacity to retain ammonia [38,39].

During the incubation of zebrafish embryos with the asparaginase, free or encapsulated, the number of live and dead embryos was recorded during 80 hpf. A significant difference in the zebrafish embryos' survival rate when incubated with Np 7 µg/mL was observed. This decrease in the toxicity could be due to the nanoparticles' capacity to retain ammonia. It was already described for *Gobiocypris rarus* (a species that shows features similarities with zebrafish) that high levels of ammonia decreased growth, retarded development and increased mortality [40]. The retention of ammonia by the nanoparticles will decrease the ammonia concentration and avoid its potentials side-effects. Increasing the survival rate observed for the zebrafish embryos. The significant effect verified at 56 hpf as an acceleration in the hatching rate for all the tested conditions could be explained as, upon hatching, the chorion is digested by event-related proteolytic enzymes, which are thought to be responsible for the chorion softening process [41]. A potential solubilization *via* ASN of minor portions of the zebrafish egg envelop glycoproteins could underlie an acceleration of chorion softening process and, thus, explain the relative increased percentage of hatched embryos. For the effect on embryos yolk extension, it was verified a significant increase in this parameter when the embryos were incubated with ASN 70 µg/mL and Np 7 µg/mL. Interestingly, the extracellular matrix protein laminin α-5 has been implicated in yolk extension formation and fins development at zebrafish trunk edges [29,42]. As for the membrane protein of zebrafish chorion, potential catalysis of ASN over asparagine residues from laminin α-5 is a reasonable assumption.

Generally, the BSA/$ASN_{25\%}$/Pol_{407} nanoparticles proved to be safe to the zebrafish embryos. The enzyme entrapment decreased the negative effect of free ASN on zebrafish survival and this formulation did

not affect the development process of zebrafish embryos in any of the tested parameters, except for the hatching rate.

5. Conclusion

A new system for the entrapment of asparaginase was successfully developed by high pressure homogenization using BSA and Pol 407 as core nanoparticle constituents. The systems with higher enzyme percentage (15, 20 and 25%) were capable to maintain the initial ASN activity for at least 4 months and in some cases, there was an increase on enzyme activity. The formulation $BSA/ASN_{25\%}/Pol_{407}$ exhibited features (size and PdI) appropriated for an intravenous application and was able to retain ammonia when compared with the free enzyme. To reduce the ammonia levels in blood, nowadays, it is used several techniques like hemodialysis capable to increase the nitrogen excretion, or therapy with sodium benzoate and sodium phenylacetate that are known nitrogen scavengers [9,43]. The $BSA/ASN_{25\%}/Pol_{407}$ nanoparticles *in vivo* toxicity was evaluated using the ZET protocol. Although a significant effect of the free ASN in the zebrafish embryonic survival was verified, this negative effect was avoided when the enzyme was immobilized into the nanoparticles, supporting the advantage of using this system instead of the free enzyme. Overall, the ZET results supported the safety of the $BSA/ASN_{25\%}/Pol_{407}$ nanoparticles using an *in vivo* model.

The $BSA/ASN_{25\%}/Pol_{407}$ nanoparticles here presented have a great potential to be used for the treatment of ALL since ASN activity is stable for a higher period of time. Moreover, the formulation has the capacity to retain the forming ammonia, which could avoid hyperammonemia. Additional studies will be performed in the future to characterize the nanoparticles antileukemic activity *in vitro* and *in vivo* using cells and animal models.

Acknowledgements

This study was supported by FCT under the scope of the strategic funding of UID/BIO/04469/2013 unit and COMPETE 2020 (POCI-01-0145-FEDER-006684) and BioTecNorte operation (NORTE-01-0145-FEDER-000004) and Nanotechnology Based Functional Solutions (NORTE-01-0145-FEDER-000019) funded by the European Regional Development Fund under the scope of Norte2020 - Programa Operacional Regional do Norte. We also acknowledge the strategic programme UID/BIA/04050/2013 (POCI-01-0145-FEDER-007569) funded by national funds through Fundação para a Ciência e a Tecnologia (FCT) and by the ERDF through the COMPETE2020 - Programa Operacional Competitividade e Internacionalização (POCI). Marisa P. Sária was supported by Marie Curie COFUND funding from the European Union's 7th Framework Programme for research, technological development and demonstration under grant agreement 600,375. Artur Ribeiro and Ana Tinoco thanks FCT for funding the scholarships with the references SFRH/BPD/98388/2013, SFRH/BD/114035/2015, respectively.

References

[1] J.M. Kwan, A.M. Fialho, M. Kundu, J. Thomas, C.S. Hong, T.K. Das Gupta, A.M. Chakrabarty, Bacterial proteins as potential drugs in the treatment of leukemia, Leuk. Res. 33 (2009) 1392–1399, https://doi.org/10.1016/j.leukres.2009.01.024.

[2] R. Jain, K.U. Zaidi, Y. Verma, P. Saxena, L-asparaginase: a promising enzyme for treatment of acute lymphoblastic leukiemia, People's J. Sci. Res. 5 (2012) 29–35.

[3] N.E. El-Naggar, S.M. El-Ewasy, N.M. El-Shweihy, Microbial L-asparaginase as a potential T therapeutic agent for the treatment of acute lymphoblastic leukemia: the pros and cons, Int. J. Pharmacol. 10 (2014) 182–199.

[4] S.-H. Chen, Asparaginase therapy in pediatric acute lymphoblastic leukemia: a focus on the mode of drug resistance, Pediatr. Neonatol. 56 (2015) 287–293, https://doi.org/10.1016/j.pedneo.2014.10.006.

[5] R.A. Egler, S.P. Ahuja, Y. Matloub, L-asparaginase in the treatment of patients with acute lymphoblastic leukemia, Cancer 117 (2016) 238–249, https://doi.org/10.4103/0976-500X.184769.

[6] E.H. Panosyan, Y. Wang, P. Xia, Asparagine depletion potentiates the cytotoxic effect of chemotherapy against brain tumors, Mol. Cancer Res. 1 (12) (2014) 694–702, https://doi.org/10.1158/1541-7786.MCR-13-0576.

[7] K. Kumar, J. Kaur, S. Walia, T. Pathak, K. Kumar, J. Kaur, S. Walia, T. Pathak, D. Aggarwal, L-asparaginase: an eff ective agent in the treatment of acute lymphoblastic leukemia, Leuk. Lymphoma 55 (2014) 256–262, https://doi.org/10.3109/10428194.2013.803224.

[8] L. Nott, T.J. Price, K. Pittman, K. Patterson, J. Fletcher, Hyperammonemia encephalopathy: an important cause of neurological deterioration following chemotherapy, Leuk. Lymphoma 48 (2007) 1702–1711, https://doi.org/10.1080/10428190701509822.

[9] S.E. Lyles, K. Kow, R.J. Milner, G.J. Buckley, C. Bandt, K.J. Baxter, Acute hyperammonemia after L-asparaginase administration in a dog, J. Vet. Emerg. Crit. Care 21 (2011) 673–678, https://doi.org/10.1111/j.1476-4431.2011.00695.x.

[10] K.M. Heitink-Pollé, B.H. Prinsen, T.J. Koning, P.M. van Hasselt, M.B. Bierings, High incidence of symptomatic hyperammonemia in children with acute lymphoblastic leukemia receiving pegylated asparaginase, JIMD Rep. Case Res. Rep. 4 (2012) 103–108, https://doi.org/10.1007/8904.

[11] A. Tinoco, A. Ribeiro, C. Oliveira, P. Parpot, A. Gomes, A. Cavaco-Paulo, Albumin/asparaginase capsules prepared by ultrasound to retain ammonia, Appl. Microbiol. Biotechnol. 100 (2016) 1–10, https://doi.org/10.1007/s00253-016-7668-4.

[12] A.O. Elzoghby, W.M. Samy, Na. Elgindy, Protein-based nanocarriers as promising drug and gene delivery systems, J. Control Release 161 (2012) 38–49, https://doi.org/10.1016/j.jconrel.2012.04.036.

[13] A. Loureiro, A.S. Abreu, M.P. Sária, M.C.O. Figueiredo, L.M. Saraiva, G.J.L. Bernardes, A.C. Gomes, A. Cavaco-Paulo, Functionalized protein nanoemulsions by incorporation of chemically modified BSA, RSC Adv. 5 (2015) 4976–4983, https://doi.org/10.1039/C4RA13802C.

[14] A. Loureiro, N.G. Azoia, A.C. Gomes, A. Cavaco-Paulo, Albumin-based nanodevices as drug carriers, Curr. Pharm. Des. 22 (2016) 1371–1390, https://doi.org/10.2174/1381612822666160125114900.

[15] A. Loureiro, E. Nogueira, N.G. Azoria, M.P. Sarria, A.S. Abreu, U. Shimanovich, A. Rollett, J. Marmark, H. Herbert, G. Guebitz, C.J. Bernardes, A. Preto, A.C. Gomes, A. Cavaco-Paulo, Size controlled protein nanoemulsions for active targeting of folate receptor positive cells, Colloids Surf. B Biointerfaces 135 (2015) 90–98, https://doi.org/10.1016/j.colsurfb.2015.06.073.

[16] M.M. Pedras, C.R.G. Pinho, aa L. Tribst, Ma. Franchi, M. Cristianini, The effect of high pressure homogenization on microorganisms in milk, Int. Food Res. J. 19 (2012) 1–5.

[17] H.H. Gustafson, D. Holt-Casper, D.W. Grainger, H. Ghandehari, D. Grainger, Nanoparticle uptake: the phagocyte problem, Nano Today 10 (2015) 487–510, https://doi.org/10.1016/j.nantod.2015.06.006.

[18] V. Schäfer, H. von Briesen, H. Rübsamen-Waigmann, A.M. Steffan, C. Royer, J. Kreuter, Phagocytosis and degradation of human serum albumin microspheres and nanoparticles in human macrophages, J. Microencapsul. 11 (1994) 261–269, https://doi.org/10.3109/02652049409040455.

[19] M. Gassmann, B. Grenacher, B. Rohde, J. Vogel, Quantifying Western blots: pitfalls of densitometry, Electrophoresis 30 (2009) 1845–1855, https://doi.org/10.1002/elps.200800720.

[20] A.L. Stecher, P.M. De Deus, I. Polikarpov, Stability of L -asparaginase: an enzyme used in leukemia treatment, Pharm. Acta Helv. 74 (1999) 1–9.

[21] D. Cappelletti, L.R. Chiarelli, M.V. Pasquetto, S. Stivala, G. Valentini, C. Scotti, Helicobacter pyloril-asparaginase: a promising chemotherapeutic agent, Biochem. Biophys. Res. Commun. 377 (2008) 1222–1226, https://doi.org/10.1016/j.bbrc.2008.10.118.

[22] A.C.N. Oliveira, M.P. Sária, P. Moreira, J. Fernandes, L. Castro, I. Lopes, M. Côrte-Real, A. Cavaco-Paulo, M.E.C.D. Real Oliveira, A.C. Gomes, Counter ions and constituents combination affect DODAX: MO nanocarriers toxicity in vitro and in vivo, Toxicol. Res. 5 (2016) 1244–1255, https://doi.org/10.1039/C6TX00074F.

[23] C.B. Kimmel, W.W. Ballard, S.R. Kimmel, B. Ullmann, T.F. Schilling, Stages of embryonic development of the zebrafish, Dev. Dyn. 203 (1995) 253–310, https://doi.org/10.1002/aja.1002030302.

[24] G. Marslin, B.F.C.C. Sarmento, G. Franklin, J.A.R. Martins, C.J.R. Silva, A.F.C. Gomes, M.P. Sária, O.M.F.P. Coutinho, A.C.P. Dias, Curcumin encapsulated into methoxy poly(ethylene glycol) poly(ε-caprolactone) nanoparticles increases cellular uptake and neuroprotective effect in glioma cells, Planta Med. 83 (2017) 434–444, https://doi.org/10.1055/s-0042-112030.

[25] C.A. MacRae, R.T. Peterson, Zebrafish as tools for drug discovery, Nat. Rev. Drug Discov. 14 (2015) 721–731, https://doi.org/10.1038/nrd4627.

[26] U. Bern, Zebrafish (Danio rerio) as a model organism for investigating endocrine disruption, Comp. Biochem. Physiol. Part C 149 (2017) 187–195, https://doi.org/10.1016/j.cbpc.2008.10.099.

[27] A.L. Rubinstein, Zebrafish assays for drug toxicity screening, Expert Opin. Drug Metab. Toxicol. 2 (2006) 231–240, https://doi.org/10.1517/17425255.2.2.231.

[28] S. Scholz, S. Fischer, U. Gündel, E. Küster, T. Luckenbach, D. Voelker, The zebrafish embryo model in environmental risk assessment - applications beyond acute toxicity testing, Environ. Sci. Pollut. Res. 15 (2008) 394–404, https://doi.org/10.1007/s11356-008-0018-z.

[29] V.C. Virta, M.S. Cooper, Structural components and morphogenetic mechanics of the zebrafish yolk extension, a developmental module, J. Exp. Zool. Part B Mol. Dev. Evol. 316 B (2011) 76–92, https://doi.org/10.1002/jez.b.21381.

[30] W.H. De Jong, W.I. Hagens, P. Krystek, M.C. Burger, A.J.A.M. Sips, R.E. Geertsma, Particle size-dependent organ distribution of gold nanoparticles after intravenous administration, Biomaterials 29 (2008) 1912–1919, https://doi.org/10.1016/j.biomaterials.2007.12.037.

[31] G. Dumortier, J.L. Grossiord, F. Agnely, J.C. Chaumeil, A review of poloxamer 407

pharmaceutical and pharmacological characteristics, Expert Rev. 23 (2006) 2709–2728, https://doi.org/10.1007/s11095-006-9104-4.
[32] C. Garcia-Galan, Á. Berenguer-Murcia, R. Fernandez-Lafuente, R.C. Rodrigues, Potential of different enzyme immobilization strategies to improve enzyme performance, Adv. Synth. Catal. 353 (2011) 2885–2904, https://doi.org/10.1002/adsc.201100534.
[33] D.-H. Zhang, L.-X. Yuwen, L.-J. Peng, Parameters affecting the performance of immobilized enzyme, J. Chem. (2013) 1–7, https://doi.org/10.1155/2013/946248 (2013).
[34] C. Gutiérrez-Lovera, A.J. Vázquez-Ríos, J. Guerra-Varela, L. Sánchez, M. de la Fuente, The potential of zebrafish as a model organism for improving the translation of genetic anticancer nanomedicines, Genes (Basel) 8 (2017) 1–20, https://doi.org/10.3390/genes8120349.
[35] B. Feldman, M. Tuchman, L. Caldovic, A zebrafish model of hyperammonemia, Mol. Genet. Metab. 113 (2014) 142–147, https://doi.org/10.1016/j.ymgme.2014.07.001.
[36] M.H. Braun, S.L. Steele, M. Ekker, S.F. Perry, Nitrogen excretion in developing zebrafish (Danio rerio): a role for Rh proteins and urea transporters, AJP Ren. Physiol. 296 (2009) F994–F1005, https://doi.org/10.1152/ajprenal.90656.2008.
[37] A.M. Zimmer, C.M. Wood, Physiological and molecular ontogeny of branchial and extra-branchial urea excretion in posthatch rainbow trout (*Oncorhynchus mykiss*), Am. J. Physiol. Integr. Comp. Physiol. 310 (2016) R305–R312, https://doi.org/10.1152/ajpregu.00403.2015.
[38] Y. Kumai, J. Harris, H. Al-Rewashdy, R.W.M. Kwong, S.F. Perry, Nitrogenous waste handling by larval zebrafish *Danio rerio* in alkaline water, Physiol. Biochem. Zool. 88 (2015) 137–145, https://doi.org/10.1086/679628.
[39] C. Bucking, C.M.R. Lemoine, P.J. Walsh, Waste nitrogen metabolism and excretion in zebrafish embryos: effects of light, ammonia, and nicotinamide, J. Exp. Zool. Part A Ecol. Genet. Physiol. 319 (2013) 391–403, https://doi.org/10.1002/jez.1802.
[40] S. Luo, W. Benli, X. Xiong, J. Wang, Short-term toxicity of ammonia, nitrite and nitrate to early life stages of the rara minnow (gobiocypris rarus), Environ. Toxicol. Chem. 35 (2016) 1422–1427, https://doi.org/10.1002/etc.3283.
[41] D. Kim, C.N. Hwang, Y. Sun, S.H. Lee, B. Kim, B.J. Nelson, Mechanical analysis of chorion softening in prehatching stages of zebrafish embryos, IEEE Trans. Nanobiosci. 5 (2006) 89–94.
[42] A.E. Webb, J. Sanderford, D. Frank, W.S. Talbot, W. Driever, D. Kimelman, Laminin alpha 5 is essential for the formation of the zebrafish fins, Dev. Biol. 311 (2007) 369–382, https://doi.org/10.1016/j.ydbio.2007.08.034.
[43] A. Auron, P.D. Brophy, Hyperammonemia in review: pathophysiology, diagnosis, and treatment, Pediatr. Nephrol. 27 (2012) 207–222, https://doi.org/10.1007/s00467-011-1838-5.